1992SvA....36..517K

least an order of magnitude from the northern to the southern end of the cloud. It is not yet clear what causes such large differences in star-forming efficiency.

[1]V. S. Shevchenko and S. D. Yakubov, *Astron. Zh.* **69**, 705 (1992) [*Sov. Astron.* **36**, 359 (1992)].
[2]V. S. Shevchenko, *Investigation of Extremely Young Star Complexes* [in Russian], FAN, Tashkent (1975), p. 3.
[3]V. S. Shevchenko, *Astron. Zh.* **56**, 297 (1979) [*Sov. Astron.* **23**, 163 (1979)].
[4]V. S. Shevchenko, *Astron. Zh.* **57**, 1162 (1980) [*Sov. Astron.* **24**, 670 (1980)].
[5]V. S. Shevchenko, *Pis'ma Astron. Zh.* **7**, 37 (1981) [*Sov. Astron. Lett.* **7**, 21 (1981).
[6]K. M. Strom, G. Newton, E. S. Strom, et al., *Astrophys. J. Suppl. Ser.* **71**, 183 (1989).
[7]P. N. Kholopov, N. N. Samus', V. P. Goranskii, et al., *General Catalog of Variable Stars* [in Russian], Nauka, Moscow (1985).
[8]B. V. Kukarkin, P. N. Kholopov, N. M. Artyukhina, et al., *New Catalog of Stars Suspected of Light Variation* [in Russian], Nauka, Moscow (1982).
[9]V. L. Straižys, *Byull. Vil'nius. Obs.*, No. 7 (1963).
[10]M. Cohen and L. V. Kuhi, *Astrophys. J. Suppl. Ser.* **41**, 743 (1979).
[11]V. S. Shevchenko, *Herbig Ae/Be Stars* [in Russian], FAN, Tashkent (1989).

Translated by Edward U. Oldham

Search for methanol masers at 44 GHz

S. V. Kalenskii, R. Bachiller, I. I. Berulis, I. E. Val'tts, J. Gomez-Gonzales, J. Martin-Pintado, A. Rodriguez-Franco, and V. I. Slysh

Astronomical Space Center, P. N. Lebedev Physics Institute, Russian Academy of Sciences; National Astronomy Center, Yebes, Spain

(Submitted July 16, 1991)
Astron. Zh. **69**, 1002–1014 (September–October 1992)

The results of a survey of young stellar objects in the $7_0-6_1A^+$ (44 GHz) methanol line are given. Three new masers have been detected, associated with cold IRAS sources in the clouds L 291 (GGC 27), L 379, and IC 1396N. Observations toward the detected masers were carried out in other methanol lines, $4_{-1}-3_0$E (36 GHz) and $1_0-0_0A^+$ (48 GHz). Masers were found at 36 GHz in GGD 27 and L 379; thermal emission at 48 GHz was detected from L 379. The relationship between methanol masers and high-velocity jets and dense disks around the central sources is discussed. A possible correlation between the presence of masers and the intensity of far-infrared emission is noted.

INTRODUCTION

Methanol in space was first detected by Ball et al.[1] toward the center of the Galaxy ($1_{10}-1_{11}A$ transition, 834 MHz). In 1971 Barrett et al.[2] detected a series of J_2-J_1E methanol lines at 25 GHz toward the Kleinmann–Low nebula, with all lines in the series being maser lines, as shown using the interferometric observations of Matsakis et al.[3] Morimoto et al.[4] detected narrow ($\Delta V < 1.5$ km/sec) "spikes" on top of broader components in the $4_{-1}-3_0E$ (36 GHz) and $7_0-6_1A^+$ (44 GHz) lines toward Sgr B2 and some other molecular clouds, and they showed that those spikes are maser lines. Subsequently, Menten et al.,[5] Haschick and Baan,[6] Norris et al.,[7] Haschick et al.,[8] and Bachiller et al.,[9] carried out a number of surveys in those and some other methanol lines. Those surveys showed that narrow (<1 km/sec) maser features, sometimes on top of broader components, are often observed in star-forming regions. Methanol masers most often emit single lines, and less often consist of several components separated in radial velocity by several km/sec. In none of the sources have high-velocity components, separated from the center by tens of km/sec, been observed.

Batrla et al.[10] have divided methanol masers into two classes, I and II. Class II includes masers in the $2_0-3_{-1}E$ (12 GHz) transition. Those masers coincide spatially with compact H II regions and pockets of OH and H_2O maser activity. This class also includes masers in the $9_2-10_1A^+$, 2_1-3_0E, $7_{-2}-8_{-1}E$, $6_2-5_3A^-$, and $6_2-5_3A^+$ transitions. Masers in class I, although they lie in star-forming regions, often do not coincide spatially with H II regions or OH masers. Class I includes masers in the $7_0-6_1A^+$, $8_0-7_1A^+$, $4_{-1}-3_0E$, and $5_{-1}-4_0E$ transitions, as well as J_2-J_1E transitions. To demonstrate the possible relationship between masers of class I and protostars and stars in early stages of evolution, we have searched for masers in the $7_0-6_1A^+$ line with the radio telescope at Yebes (Spain) in the following objects.

1) Cold IRAS sources in Orion and Cepheus, toward which Wouterloot et al.[11] have sought ammonia lines (henceforth catalog I). In those sources, the flux S_{60} at 60 μm is greater than S_{25} at 25 μm and/or $S_{25} > S_{12}$. We selected for observation only those sources toward which emission in NH_3, CO, or H_2O lines has been detected in Refs. 11-13, a total of 79 objects.

2) IRAS sources in Cygnus and Cepheus, toward which Guilbudaghian et al.[14] sought H_2O masers (14 out of 21 objects, catalog II).

3) Cold IRAS sources not identified in the optical range,

 0038-5301/92/05 0517-07 $03.00 © 1993 American Institute of Physics

© American Institute of Physics • Provided by the NASA Astrophysics Data System

1992SvA....36..517K

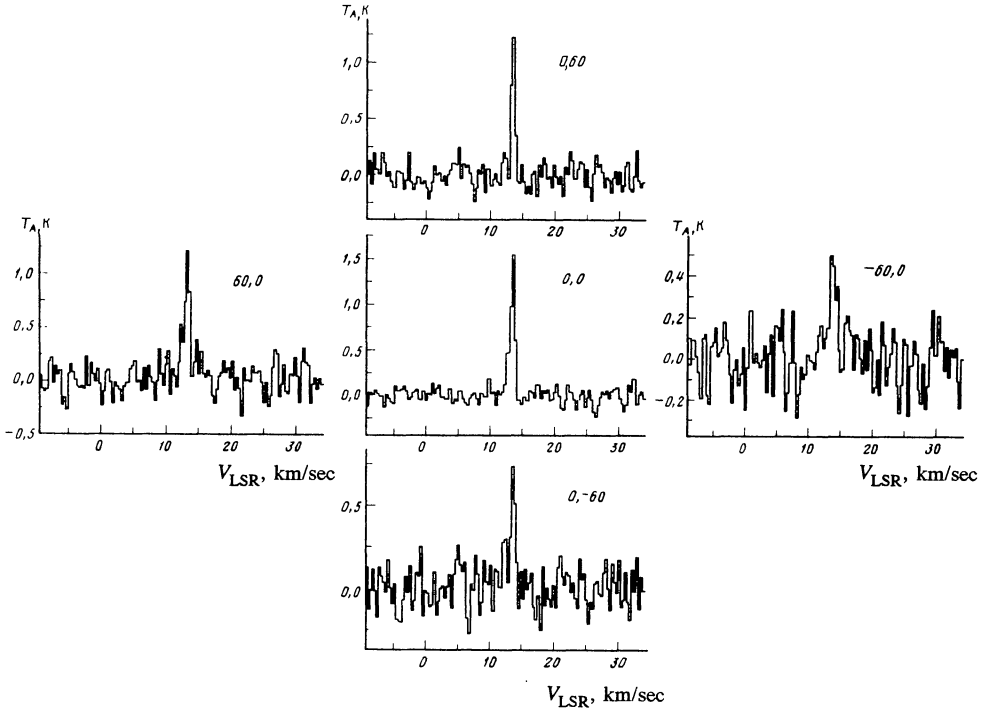

FIG. 1. Spectra of GGD 27 in the $7_0-6_1A^+$ methanol line.

from the list of Wilking et al.[15] For these sources $S_{60} \geq 100$ Jy and $S_{100} \geq S_{60}$ (catalog III, 41 out of 50 sources).

4) Ultracompact H II regions from the list of Wood and Churchwell[16] (nine objects) and that of Churchwell et al.[17] (three objects).

We also took sources from Weintraub's catalog[18] of emission-line stars in the pre-main-sequence stage (two sources) and from the catalog of H_2O maser sources of Cesaroni et al.[19] (three sources).

In three cold IRAS sources from catalog III (one of which also appears in catalog II), new masers were detected in the $7_0-6_1A^+$ line, which we then investigated in the $1_0-0_0A^+$ (48 GHz) line and, with the RT-22 telescope of the P. N. Lebedev Physics Institute, Russian Academy of Sciences (FIAN), in the $4_{-1}-3_0E$ (36 GHz) line. Maser lines at 36 GHz were detected in two sources.

OBSERVATIONS

Observations in the $7_0-6_1A^+$ (44.06943 GHz) and $1_0-0_0A^+$ (48.37246 GHz) transitions were carried out with the 14-m radio telescope of the Astronomy Center at Yebes (Spain) from 13 to 25 January and from 8 to 14 April 1991. Observations in the $4_{-1}-3_0E$ (36.16924 GHz) line were carried out with the 22-m radio telescope of the Radio Astronomy Station at the Astronomical Center of the FIAN at Pushchino. The Spanish telescope is equipped with a receiver having a cooled mixer based on Schottky barrier diodes. The system's noise temperature varied as a function of weather and source elevation: in the range 70-100 K at 44 GHz and 100-130 K at 48 GHz. One kelvin of antenna temperature corresponds to a flux 90 Jy. The antenna beamwidth is 2′. The efficiency of the main lobe of the beam pattern is 0.43. The telescope pointing accuracy is 20″. The spectrometer is a 256×50 kHz filter bank, which corresponds to 0.34 km/sec resolution at 44 GHz and 0.32 km/sec at 48 GHz. The observations were carried out in frequency-switched mode.

The Pushchino telescope in the 36 GHz range is equipped with a maser amplifier. The system's noise temperature varied in the 250-300 K range. One kelvin of antenna temperature at 36 GHz corresponds to a flux 40 Jy. The antenna beamwidth is 2′ and the antenna pointing accuracy is 30″. The observations were carried out with a 32×125 kHz filter-bank spectrum analyzer, which corresponds to a velocity resolution 1.04 km/sec. The source L 379 was also observed with a 96-channel filter-bank spectrometer with 7.5 kHz resolution (0.062 km/sec). All observations were carried out in beam-switching mode.

NEW MASERS

In Table I we give the parameters of the sources detected at 44, 36 and 48 GHz. A list of the sources in which no ma-

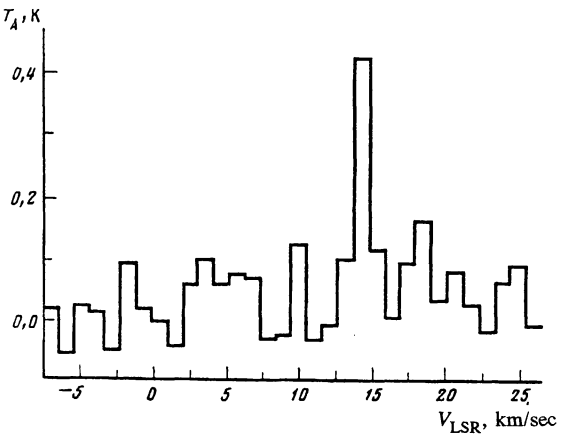

FIG. 2. Spectrum of GGD 27 in the $4_{-1}-3_0E$ methanol line.

© American Institute of Physics • Provided by the NASA Astrophysics Data System

1992SvA....36..517K

TABLE I. Parameters of the Detected Sources

Source	$\alpha_{1950}\ \delta_{1950}$	Trans.	T_A, K	V_{LSR}, km/sec	ΔV*, km/sec	S_ν, Jy
GGD 27	$18^h16^m13^s,8$	$7_0 - 6_1A^+$	1,50	13,5 ± 0,1	0,8	135
	$-20°48'31''$	$4_{-1} - 3_0E$	0,43	14,0 ± 0,5	<1	17
		$1_0 - 0_0A^+$	<0,1			<9
L 379	$18^h26^m32^s,9$	$7_0 - 6_1A^+$	0,70 **	18,0 ± 0,1	1,1	63
	$-15°17'51''$		0,50	19,0 ± 0,1	3,3	45
		$4_{-1} - 3_0E$	0,88	18,0 ± 0,2	1,9	36
			0,96	20,4 ± 0,2	1,2	38
		$1_0 - 0_0A^+$	0,13	18,6 ± 0,1	5,1	12
IC 1396N	$21^h39^m10^s,3$	$7_0 - 6_1A^+$	0,14	−0,5 ± 0,1	0,6	15
	$58°02'29''$	$4_{-1} - 3_0E$	<0,15			<6
		$1_0 - 0_0A^+$	<0,1			<9

*The line width has not been corrected for the spectrometer resolution.

**The coordinates of the first component are shifted relative to the IRAS source by $-30''$ in α and $+30''$ in δ.

sers were found at 44 GHz is given in Table II. Below we describe the three regions in which new masers were detected.

GGD 27. A narrow (ΔV = 0.8 km/sec)[1)] and strong (S_ν = 135 Jy) line in the $7_0-6_1A^+$ transition was detected toward the cold source IRAS 18162−2048 (GGD 27 IRS2). Mapping of the source (Fig. 1) showed that it is unresolved and has an angular size less than 2′. Its coordinates are α_{1950} = $18^h16^m13^s.8 \pm 1^s.3$ and $\delta_{1950} = -20°48'31'' \pm 20''$. A narrow line coinciding in radial velocity with the line at 44 GHz was also detected in the $4_{-1}-3_0E$ transition (Fig. 2). Unfortunately, the parameters of the line could not be determined accurately because of insufficient spectral resolution. No emission in the $1_0-0_0A^+$ line was detected at the 0.2 K level in brightness temperature averaged over the main lobe of the beam pattern.

The source GGD 27 IRS2 is the central source of a bipolar jet[21,22] with a dense disk extending perpendicular to the jet axis. Rodriguez et al.[20] had earlier detected a compact radio continuum source at 5 GHz (coinciding with GGD 27 IRS2 to within the aiming errors) and OH and H_2O masers associated with it. The 44 GHz methanol maser is projected onto the dense disk and coincides with IRAS 18162−2048 to within the observational errors (Fig. 3). The radial velocity of the 44 GHz and 36 GHz masers coincides approximately with that of the disk and the quiescent gas in the cloud, determined by Yamashita et al.[22]

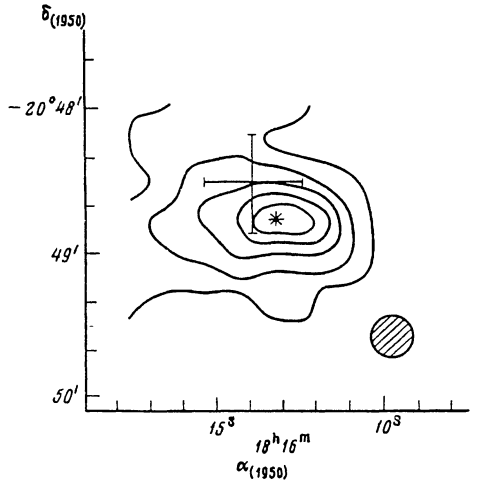

FIG. 3. Map of the gaseous disk of GGD 27 in the 2−1 CS line from Yamashita et al.[22] The position of the infrared source is denoted by an asterisk and that of the maser in the $7_0-6_1A^+$ line by a cross.

An upper limit on the methanol column density in the disk can be determined from observations of thermal emission in the $1_0-0_0A^+$ line. The disk's dimensions[22] are $60''\times30''$; for a telescope beamwidth 2′, the dilution factor is 0.125, and the upper limit on the disk's brightness temperature in the $1_0-0_0A^+$ line is 1.6 K. Assuming a small optical depth and taking a rotational temperature 40 K (equal to the CS excitation temperature), we obtain a methanol column density $\leq 10^{15}$ cm^{-2}, which at a hydrogen column density 10^{23} cm^{-2} leads to a methanol abundance $\leq 10^{-8}$.

L 379. A strong, asymmetric line, whose shape varies from point to point (Fig. 4), was detected at the frequency of the $7_0-6_1A^+$ methanol transition toward the cold source IRAS 18265−1517, located in the dark cloud L 379. The lack of symmetry and the different shapes of the spectrum at different points indicate that the source consists of several components that do not coincide spatially. The observed spectrum at the point (−60″, 0″) can be represented by a Gaussian profile with parameters T_A = 0.6 K, V_{LSR} = 18.2 km/sec, and ΔV = 1.1 km/sec, while that at (60″, 0″) can be represented by a Gaussian with T_A = 0.24 K, V_{LSR} = 19.0 km/sec, and ΔV = 2.7 km/sec.

The source can be modeled as a sum of two components: a "narrow" point component with line parameters T_A = 0.7 K, V_{LSR} = 18.1 km/sec, and ΔV = 1.1 km/sec, located at a distance (−30″, 30″) from IRAS 18265−1517, and a "broad" component, possibly also a point source, with V_{LSR} = 19 km/sec and ΔV = 3 km/sec and with a peak brightness T_A = 0.5 K, which coincides with IRAS 18265−1517. Unfortunately, there are no observations south of the brightness peak of the second source, which precludes a reliable determination of its size. Moreover, because of strong blending of features in the spectra, the given resolution cannot be considered entirely reliable. Observations with higher angular resolution are needed to reveal the source's true structure.

A two-humped line with a narrow (1.2 km/sec), probably maser feature at 20.4 km/sec and a broader component (1.9

© American Institute of Physics • Provided by the NASA Astrophysics Data System

1992SvA....36..517K

TABLE II. Sources from which No Emission at 44 GHz Was Detected at the 10 Jy Level

IRAS	α_{1950}	δ_{1950}	V_{LSR}*, km/sec	Other names
00070 + 6503	$00^h07^m04^s6$	65°03′28″	−64	
00211 + 6549	00 21 09,6	65 49 26	−69	
00412 + 6638	00 41 12,6	66 38 16	0	
00468 + 6527	00 46 51,2	65 27 19	−64	
00484 + 6531	00 48 27,3	65 31 40	−64	
00554 + 6524	00 55 29,0	65 24 31	−63	
01045 + 6505	01 04 35,7	65 05 21	−88	
02383 + 6241	02 38 22,8	62 41 05	−71	
02575 + 6017	02 57 35,6	60 17 21	−35	
03035 + 5819	03 03 33,2	58 19 20	−40	HHL-5
04287 + 1801	04 28 43,8	18 01 51	7	L 1551-IRS5
04535 + 3752	04 53 30,8	37 52 32	−36	
04579 + 4703	04 57 56,6	47 03 03	−17	
05311 — 0631	05 31 06,3	−06 31 45	6	
05329 — 0628	05 32 59,4	−06 28 49	9	
05338 — 0624	05 33 52,7	−06 24 02	7	L 1641N
05340 — 0603	05 34 01,5	−06 03 06	8	
05357 — 0650	05 35 43,8	−06 50 56	8	
05358 — 0704	05 35 53,3	−07 04 07	5	
05358 + 3543	05 35 48,8	35 43 41	−17	S 231
05361 + 3539	05 36 06,4	35 39 21	−16	
05363 — 0702	05 36 20,9	−07 02 43	4	
05369 — 0728	05 36 56,4	−07 28 14	4	
05373 + 2349	05 37 21,3	23 49 22	3	GGD 4
05375 — 0731	05 37 31,1	−07 31 59	5	L 1641S
05378 — 0750	05 37 52,1	−07 50 04	5	
05379 — 0758	05 37 56,1	−07 58 03	5	
05380 — 0728	05 38 02,7	−07 28 59	5	R 50
05384 — 0808	05 38 24,6	−08 08 20	6	
05385 — 0247	05 38 35,7	−02 47 43	6	
05387 — 0924	05 38 42,4	−09 24 46	3	
05389 — 0756	05 38 59,3	−07 56 40	5	
05391 — 0217	05 39 06,8	−02 17 18	10	
05393 — 0156	05 39 18,0	−01 56 42	11	
05394 — 0253	05 39 24,3	−02 53 26	6	
05399 — 0121	05 39 55,5	−01 21 24	9	
05400 — 0800	05 40 00,7	−08 00 13	9	
05403 — 0818	05 40 23,3	−08 18 26	3	
05404 — 0948	05 40 25,5	−09 48 44	3	
05404 — 0220	05 40 29,1	−02 20 05	9	
05405 — 0117	05 40 30,3	−01 17 43	9	
05413 — 0104	05 41 18,6	−01 04 17	2	
05427 — 0116	05 42 43,8	−01 16 45	2	
05435 — 0015	05 43 31,1	−00 15 28	11	
05437 — 0001	05 43 44,1	−00 01 23	9	
05445 + 0020	05 44 30,3	00 20 17	9	NGC 2071
05450 + 0019	05 45 00,5	00 19 08	9	
05451 + 0037	05 45 07,8	00 37 41	9	
05462 — 0124	05 46 13,1	−01 24 42	9	
06103 — 0612	06 10 21,8	−06 12 28	0	Bretz 4
	06 10 23,0	−06 12 55	7	HH 16—17
06249 — 1007	06 24 56,2	−10 07 47	12	
06291 + 0421	06 29 09,3	04 21 44	13	Mon OB2
06308 + 0442	06 30 52,7	04 02 27	15	RNO 73
06572 — 0742	06 57 16,8	−07 42 16	0	NGC 2316 N
	07 22 33,4	−24 28 58	24	HHL-50
07277 — 1821	07 27 43,2	−18 21 41	42	
	07 30 47,6	30 37 13	4	AFGL 1141
18021 — 1950?	18 02 15,2	−19 50 51	0	G 10.10 + 0.74
18056 — 1952	18 05 40,27	−19 52 20,7	0; 64	G 10.47 + 0.03 Complex
18099 — 1810	18 09 58,9	−18 11 58,4	0	G 12.43 — 0.05
18123 — 1203	18 12 19,3	−12 03 42	33	S 54
18141 — 1156	18 14 08,1	−11 56 02	30	S 54
18151 — 1134	18 15 09,6	−11 34 40	28	S 54
18319 — 0834	18 32 01,2	−08 33 32,9	0; 70	G 23.46 — 0.20
	18 47 57,0	−00 05 34,0	16	G 32.8 + 0.19
18496 + 0004	18 49 34,0	00 04 30	76	
18502 + 0051	18 50 17,5	00 51 45,8	0	G 33.92 + 0.11
18503 + 0051	18 50 16,3	00 51 45	108	
18515 + 0157	18 51 29,5	01 57 43	53	
19048 + 0745	19 04 44,8	07 46 51,6	0	G 41.71 + 0.11
19048 + 0748	19 04 50,5	07 47 59	0	G 41.74 + 0.10
19054 + 0901	19 05 18,4	09 02 25,6	0	G 42.90 + 0.57 Complex
19074 + 0814	19 07 25,0	08 13 48	0	G 42.42 — 0.27 Complex
20050 + 2720	20 05 02,5	27 20 09	6	Cyg Rift
20081 + 2720	20 08 07,0	27 20 11	6	Cyg Rift
20126 + 4104	20 12 41,0	41 04 20	−4	Cyg X
20178 + 4046	20 17 53,0	40 47 00	1	Cyg X
20190 + 4102	20 19 01,2	41 02 35	3	Cyg X
20216 + 4107	20 21 37,6	41 07 56	−1	Cyg X
20227 + 4154	20 22 46,3	41 54 29	6	Cyg X
20228 + 4215	20 22 49,9	42 15 13	5	Cyg X
20275 + 4001	20 27 36,0	40 01 16	−6	
20278 + 3521	20 27 51,0	35 21 33	−4	Cyg X
21015 + 5918	21 01 33,9	59 18 53	−80	
21046 + 5110	21 04 40,0	51 10 08	−1	Cyg OB7
21078 + 5211	21 07 50,2	52 11 29	−6	Cyg OB7
21144 + 5430	21 14 24,1	54 30 57	−88	
21173 + 5450	21 17 21,2	54 50 39	−82	
21184 + 5507	21 18 26,9	55 07 07	0; −80	
21246 + 5512	21 24 40,9	55 12 54	0; −60	

© American Institute of Physics • Provided by the NASA Astrophysics Data System

1992SvA....36..517K

TABLE II *(continued)*

IRAS	α_{1950}	δ_{1950}	V_{LSR}*, km/sec	Other names
21336 + 5333	21 33 41,1	53 33 45	0; −70	
21340 + 5399	21 34 04,1	53 39 31	0; −70	
21368 + 5456	21 36 52,3	54 56 47	−57	
21388 + 5622	21 38 53,2	56 22 18	−4	
21413 + 5442	21 41 21,2	54 42 30	−70	
21418 + 5403	21 41 48,2	54 03 09	0; −70	
21561 + 5806	21 56 06,0	58 06 45	−71	
22036 + 6034	22 03 38,8	60 34 04	−70	
22147 + 5948	22 14 45,6	59 48 49	−60	
22198 + 6336	22 19 50,7	63 36 33	−11	S 140
22272 + 6358A	22 27 12,2	63 58 21	−9	S 140
22444 + 5827	22 44 25,7	58 27 29	−3	
22451 + 6154	22 45 08,2	61 54 21	−9	
22452 + 5835	22 45 16,1	58 35 33	−0	
22453 + 5740	22 45 22,0	57 40 04	−10	
22457 + 6146	22 45 23,3	61 46 07	−10	
22475 + 5939	22 47 30,9	59 39 03	−51	
22506 + 5944	22 50 37,9	59 44 50	−51	
22512 + 6201	22 51 14,1	62 01 23	−8	
22517 + 6215	22 51 43,7	62 16 00	−9	
22528 + 5936	22 52 49,6	59 36 40	−53	
22539 + 5758	22 53 56,0	57 58 48	−54	
22542 + 5815	22 54 13,5	58 15 11	−52	
22544 + 5808	22 54 27,8	58 08 50	−55	
22566 + 5830	22 56 38,3	58 31 40	−50	
	22 56 45,2	58 29 10	−51	S 152OH
22570 + 5912	22 57 02,8	59 12 22	−46	
22598 + 5846	22 59 53,6	58 46 15	−48	
23011 + 6126	23 01 10,9	61 26 11	−10	
23026 + 5948	23 02 40,0	59 48 23	−51	
23030 + 5958	23 03 04,9	59 58 28	−53	
23032 + 5937	23 03 16,9	59 37 40	−51	
23033 + 5951	23 03 19,7	59 51 55	−53	
23037 + 6213	23 03 46,7	62 13 59	−9	
23045 + 6215	23 04 31,0	62 15 17	−8	
23071 + 6033	23 07 07,0	60 33 01	−52	
23103 + 6109	23 10 21,6	61 09 16	−55	
23116 + 6111	23 11 36,6	61 11 48	−57	
23125 + 5921	23 12 33,0	59 21 08	−45	
23133 + 6050	23 13 21,5	60 50 47	−56	
23136 + 6111	23 13 40,3	61 11 47	−53	
23138 + 5945	23 13 53,5	59 45 37	−44	
23139 + 5939	23 13 57,9	59 39 00	−44	
23140 + 6121	23 14 01,9	61 21 22	−52	
23146 + 5954	23 14 37,4	59 54 23	−48	
23151 + 5912	23 15 10,1	59 12 11	−55	
23185 + 6055	23 18 30,6	60 55 24	−55	
23239 + 5826	23 23 57,5	58 26 19	−55	
23250 + 5837	23 25 00,9	58 38 13	−55	
23545 + 6508	23 54 34,1	65 08 29	−19	S 171
23568 + 6706	23 56 53,3	67 06 57	−13	S 171

*Analysis bandwidth 43 km/sec, centered at the radial velocity given in the table.

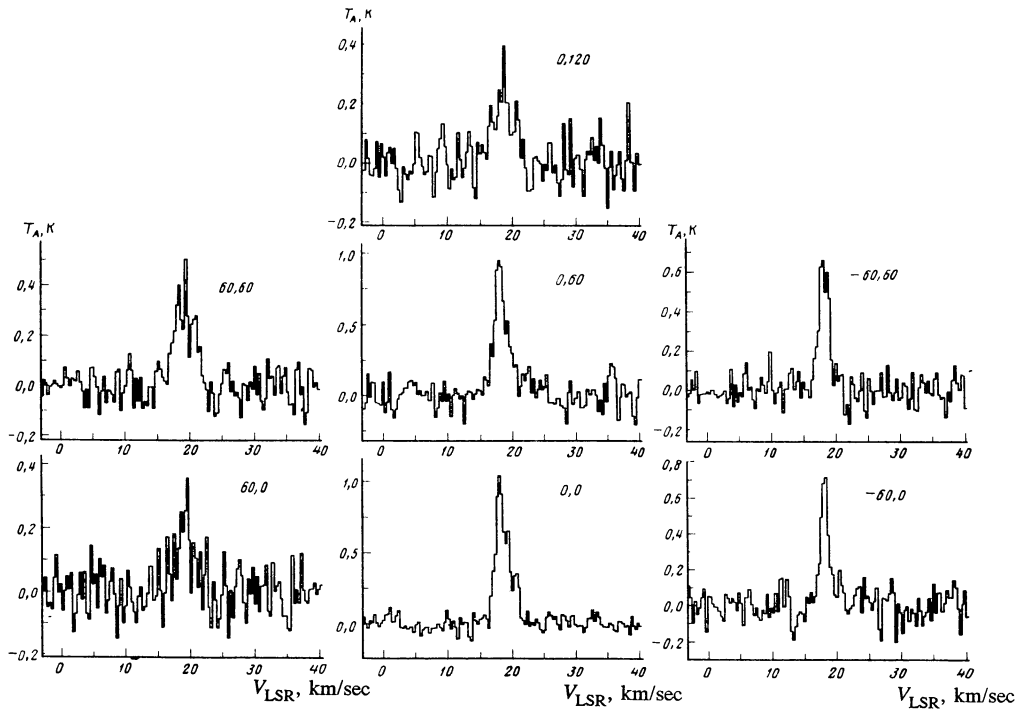

FIG. 4. Spectra of L 379 in the $7_0-6_1A^+$ methanol line.

© American Institute of Physics • Provided by the NASA Astrophysics Data System

1992SvA....36..517K

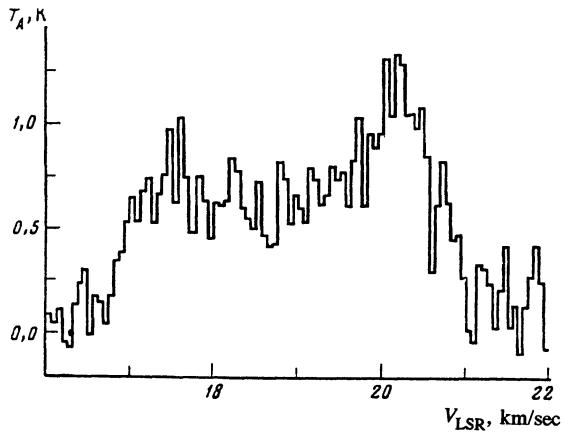

FIG. 5. Spectrum of L 379 in the $4_{-1}-3_0E$ methanol line.

km/sec) at 18 km/sec, was detected in the $4_{-1}-3_0E$ transition toward IRAS 18265−1517 (Fig. 5). That feature coincides in radial velocity with the narrow component at 44 GHz. Methanol thermal emission was detected in the $1_0-0_0A^+$ line toward IRAS 18265−1517 (Fig. 6).

Hilton et al.[23] have mapped the cloud in the 2−1 CO line and discovered a bipolar jet, the central source of which is IRAS 18265−1517. A "hot spot" with a diameter ~2′ was also found (Fig. 7). IRAS 18265−1517 approximately coincides with the brightness maximum of the spot, which may consist of a dense disk around the central source. The components of the methanol source coincide in coordinates with the dense disk and their location is shown by crosses in Fig. 7.

Thus, in L 379, just as in GGD 27, the methanol masers are located near the central source of a bipolar jet, and are probably projected onto the central dense disk.

Since the methanol rotational temperature equals the kinetic temperature of the gas, which is 18 K toward the "hot spot,"[23] from the brightness temperature 0.3 K of the $1_0-0_0A^+$ line we can determine the methanol column density, which turns out to be $7\cdot10^{14}$ cm^{-2}.

IC 1396N. A narrow (ΔV = 0.6 km/sec) methanol maser line in the $7_0-6_1A^+$ transition was detected at radial velocity −0.5 km/sec (Fig. 8) toward the cold source IRAS 21391+5802 in the globule IC 1396N. No emission at 36 GHz was detected at the 6 Jy level. An upper limit of 0.2 K was

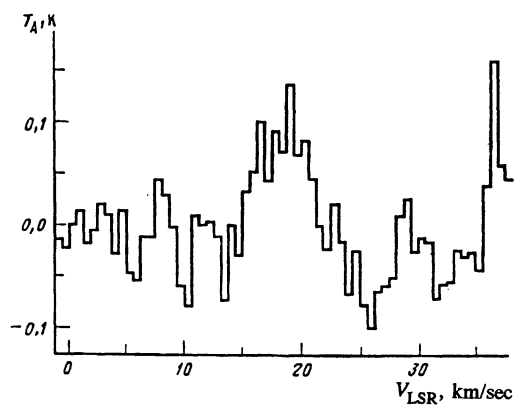

FIG. 6. Spectrum of L 379 in the $1_0-0_0A^+$ methanol line.

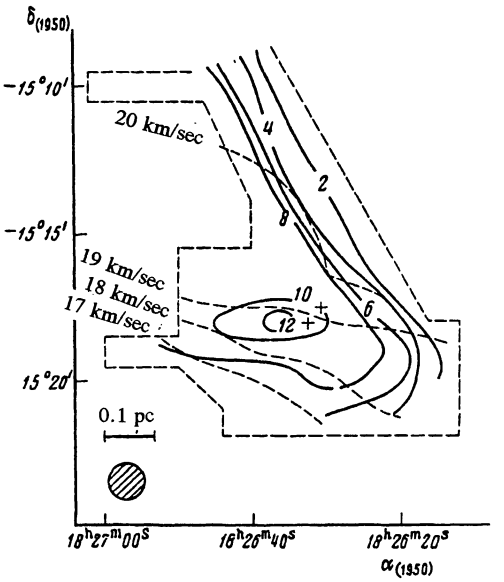

FIG. 7. Map of L 379 in the 2−1 CO line from Hilton et al.[23] The positions of components of the source in the $7_0-6_1A^+$ line are shown by crosses.

obtained for the brightness temperature of the globule's emission in the $1_0-0_0A^+$ line.

Sugitani et al.[24] have investigated IC 1396N in CO and ^{13}CO lines and discovered a bipolar jet, in which IRAS 21391+5802 is the central source. Guilbudaghian et al.[14] have detected an H_2O maser toward IRAS 21391+5802, and Wilking et al.[25] have detected emission in the 5−4 CS line, which may indicate the presence of a dense disk.

An upper limit on the methanol column density in the cloud for gas temperatures in the range 10-30 K has been calculated from observations of thermal emission in the $1_0-0_0A^+$ line. The respective values were $(1\text{-}6)\cdot10^{14}$ cm^{-2}. The cloud's density and mass given by Sugitani et al.[24] correspond to an H_2 column density $6\cdot10^{23}$ cm^{-2}, which yields an upper limit of $(0.2\text{-}1)\cdot10^{-9}$ for the methanol abundance.

DISCUSSION

Three new methanol maser sources have been detected toward cold IRAS sources, surrounded by heavy gas−dust shells, from catalog III, which are centers of bipolar jets and

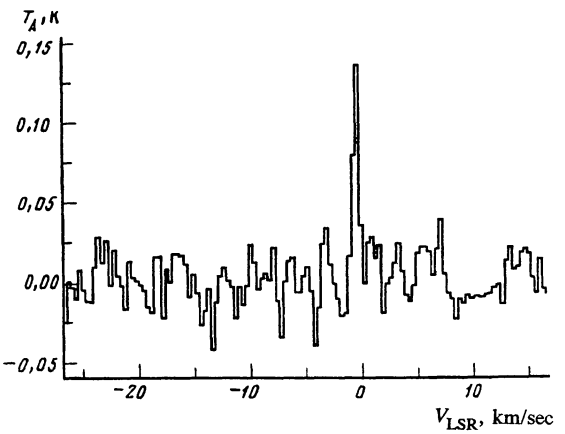

FIG. 8. Spectrum of IC 1396N in the $7_0-6_1A^+$ methanol line.

© American Institute of Physics • Provided by the NASA Astrophysics Data System

1992SvA....36..517K

may be associated with dense disks. Three other sources from the same catalog are also associated with already known methanol masers in the $7_0-6_1A^+$ line, and all three are also centers of bipolar jets. Plambeck and Menton[26] note the relationship between the methanol masers in DR 21 and high-velocity jets. The maser at 44 GHz in OMC-1 may also be associated with a high-velocity jet.[8] Bachiller et al.[9] have detected a methanol maser at 44 GHz toward the compact H II region G5.89−0.39, which is the center of a strong bipolar jet. No methanol masers were detected in any of the 25 sources from catalog III that are not associated with high-velocity jets.

A comparison of the catalogs of 44 GHz masers in Refs. 8 and 9 with Fukui's more complete catalog of high-velocity jets[27] shows that another seven high-velocity jets are associated with methanol masers. The central sources of four of them are cold ($S_{100} > S_{60}$) IRAS sources; the flux at 60 μm from three of the central sources exceeds their flux at 100 μm; the central source of the bipolar jet in DR 21 OH is probably a very cold object, with an appreciable flux only in the radio continuum.[28]

It should be noted that most of the IRAS objects associated with methanol masers are strong sources at 60 and 100 μm; thus, only one source out of all of the methanol masers in the cloud OMC-2 has a flux of 22 Jy at 100 μm; the flux from IC 1396N is 410 Jy; the fluxes from the other sources are about 1000 Jy. There may be a correlation between the luminosity of central sources and the power of methanol masers.

Such a relationship between the intensity of the central IR sources and the presence of methanol masers enables us to understand why new masers were not detected from objects in catalog I and only one new maser was detected from objects in catalog II, although sample observations of sources in catalog I in the 1−0 CO line by Wouterloot and Walmsley[13] showed that many of them are associated with high-velocity jets. Among the objects in catalog I, only 14 of the sources have a flux at 100 μm exceeding 1000 Jy; masers at 44 GHz had already been detected in two of them. Only one source in catalog II has a flux at 100 μm that exceeds 1000 Jy. The reason why only one maser has been detected is therefore the same as for catalog I.

All of the foregoing leads us to believe that the conditions for the development of methanol masers at 44 GHz exist near young stars with massive gas−dust shells that are sources of high-velocity bipolar jets and are associated with dense disks. In this connection it is of interest to search for high-velocity streams and dense disks toward methanol masers and to search for new masers toward high-velocity streams with cold central sources.

We wish to thank H. Alcolea, A. Barsia, and P. Planesasu, as well as the entire staff of the observatories at Yebes and Pushchino for assistance in preparing for and performing the observations and in data processing.

[1)]Here and below, the line width has not been corrected for the spectrometer resolution.

[1]J. A. Ball, V. A. Gottlieb, A. E. Lilley, and H. E. Radford, *Astrophys. J.* **162**, L203 (1970).
[2]A. H. Barrett, P. R. Schwartz, and J. W. Waters, *Astrophys. J.* **168**, L101 (1971).
[3]D. N. Matsakis, A. C. Cheung, M. C. Wright, et al., *Astrophys. J.* **236**, 481 (1980).
[4]M. Morimoto, M. Ohishi, and T. Kanzawa, *Astrophys. J.* **288**, L11 (1985).
[5]K. M. Menten, C. M. Walmsley, C. Henkel, and T. L. Wilson, *Astron. Astrophys.* **157**, 318 (1986).
[6]A. D. Haschick and W. A. Baan, *Astrophys. J.* **339**, 949 (1989).
[7]R. P. Norris, J. L. Caswell, F. F. Gardner, and K. J. Wellington, *Astrophys. J.* **326**, L159 (1987).
[8]A. D. Haschick, K. M. Menten, and W. A. Baan, *Astrophys. J.* **354**, 556 (1990).
[9]R. Bachiller, K. M. Menten, J. Gomez-Gonzalez, and A. Barcia, *Astron. Astrophys.* **240**, 116 (1990).
[10]W. Batrla, H. K. Matthews, K. M. Menten, and C. M. Walmsley, *Nature (London)* **326**, 49 (1987).
[11]J. G. A. Wouterloot, C. M. Walmsley, and C. Henkel, *Astron. Astrophys.* **203**, 367 (1988).
[12]J. G. A. Wouterloot, C. Henkel, and C. M. Walmsley, *Astron. Astrophys.* **215**, 131 (1989).
[13]J. G. A. Wouterloot and C. M. Walmsley, *Astron. Astrophys.* **168**, 237 (1986).
[14]A. L. Guilbudaghian, L. F. Rodriguez, and S. Curiel, *Rev. Mex. Astron. Astrofis.* **20**, 51 (1990).
[15]B. A. Wilking, L. G. Mundy, J. H. Blackwell, and J. E. Howe, *Astrophys. J.* **345**, 257 (1989).
[16]D. O. S. Wood and E. Churchwell, *Astrophys. J. Suppl. Ser.* **69**, 831 (1989).
[17]E. Churchwell, C. M. Walmsley, and R. Cesaroni, *Astron. Astrophys. Suppl. Ser.* **83**, 119 (1990).
[18]D. A. Weintraub, *Astrophys. J. Suppl. Ser.* **74**, 575 (1990).
[19]R. Cesaroni, F. Palagi, M. Felli, et al., *Astron. Astrophys. Suppl. Ser.* **76**, 445 (1988).
[20]L. F. Rodriguez, J. M. Moran, P. T. P. Ho, and E. W. Gottlieb, *Astrophys. J.* **235**, 845 (1980).
[21]T. Yamashita, S. Sato, T. Nagata, et al., *Astron. Astrophys.* **177**, 258 (1987).
[22]T. Yamashita, H. Suzuki, N. Kaifu, and M. Tamura, *Astrophys. J.* **347**, 894 (1989).
[23]J. Hilton, G. J. White, N. J. Cronin, and R. Rainey, *Astron. Astrophys.* **154**, 274 (1986).
[24]K. Sugitani, Y. Fukui, A. Mizuno, and N. Ohashi, *Astrophys. J.* **342**, L87 (1989).
[25]R. D. Schwartz, A. L. Guilbudaghian, and B. A. Wilking, *Astrophys. J.* **370**, 263 (1991).
[26]R. L. Plambeck and K. M. Menten, *Astrophys. J.* **364**, 555 (1990).
[27]Y. Fukui, in: *On Low-Mass Star Formation and Pre-Main Sequence Objects. ESO Conference Workshop No. 33, Proceedings*, Eur. Southern. Obs. (1989), p. 95.
[28]W. P. Woody, S. L. Scott, N. Z. Scoville, et al., *Astrophys. J.* **337**, L41 (1989).

Translated by Edward U. Oldham

© American Institute of Physics • Provided by the NASA Astrophysics Data System